High Current Density, Long Life Cathodes for High Power RF Sources

Final Report

Calabazas Creek Research, Inc.
690 Port Drive
San Mateo, CA 94404
(650) 312-9575, Fax: (650) 312-9536
RLI@CalCreek.com

Principle Investigator: Dr. R. Lawrence Ives

Grant Number: DE-SC0004570

1. Introduction

This program was tasked with improving the quality and expanding applications for Controlled Porosity Reservoir (CPR) cathodes. Calabazas Creek Research, Inc. (CCR) initially developed CPR cathodes on a DOE-funded SBIR program to improve cathodes for magnetron injection guns (MIGs) [1, 2]. Subsequent funding was received from the Defense Advanced Research Projects Agency (DARPA) [3]. The program developed design requirements for implementation of the technology into high current density cathodes for high frequency applications [4]. During Phase I of this program, CCR was awarded the prestigious 2011 R&D100 award for this technology [5]. Subsequently, the technology was presented at numerous technical conferences. A patent was issued for the technology in 2009 [6]. These cathodes are now marketed by Semicon Associates, Inc. in Lexington, KY. They are the world's largest producer of cathodes for vacuum electron devices.

During this program, CCR teamed with Semicon Associates, Inc. (Semicon) and Ron Witherspoon, Inc. (RWI) to improve the fabrication processes and expand applications for the cathodes. Specific fabrications issues included the quality of the wire winding that provides the basic structure and the sintering to bond the wires into a robust, cohesive structure. The program also developed improved techniques for integrating the resulting material into cathodes for electron guns.

Accomplishments in the Phase II tasks are described below.

2. Phase II Work Plan

Results from the Phase II program are described below for each of the proposed tasks.

2.1. Refine emitter design equations and experimentally verify

CPR cathodes are fabricated by winding tungsten wire around a molybdenum form and sintering [2]. The resultant structure is solid tungsten with hexagonal arrays of pores penetrating through the structure. Cathode emitters are formed by slicing the material perpendicular to the pore axis, providing an emission surface as shown in Figure 1. The sliced material forms a cap over a reservoir of work function reducing material. When heated to operating temperature, the work function reduc-

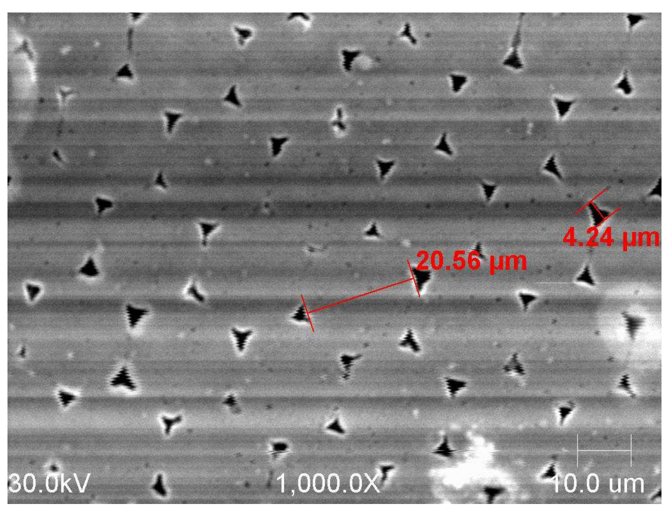

Figure 1. Sliced and polished cross section of sintered 20-micron diameter wire cathode used in CPR cathodes

ing material diffuses through the pores through Knudsen Flow to the emission surface. For thermionic cathodes, the work function reducing material is usually a mixture of barium oxide, calcium oxide, and aluminum oxide. For photocathodes, it is cesium chromate.

The diffusion rate depends on several factors, including the volatility of the material, temperature, pore size and shape, and material thickness. Jensen et al provided a basic description of the mechanisms [7], and Pan et al extended this research at the University of Maryland [8]. CCR implemented the resultant formulation into a graphical design tool for cathode design. The equations consider the specific pore geometry in CPR material and incorporate equations to calculate the temperature required to achieve a specific emission current density. The calculation provides the material thickness required to balance evaporation from the emission surface. This ensures that sufficient work function material is maintained on the surface but avoids excessive diffusion that contaminates adjacent surfaces.

Figure 2 shows the user interface for the CPR cathode design tool. User inputs include:

- Cathode size,
- Wire size,
- Current density,
- Reservoir volume.

The design tool calculates:

- Cathode temperature,
- Emitter thickness providing diffusion rate to maintain monolayer coverage,
- Estimated lifetime.

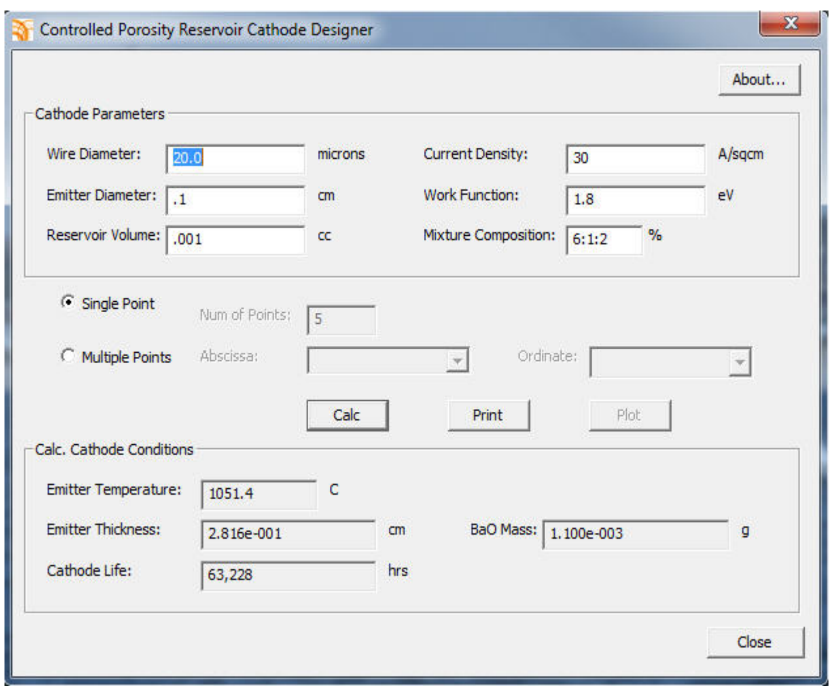

Figure 2. Controlled Porosity Reservoir Cathode Designer

This provides cathode designers sufficient information to design the cathode heater, cathode geometry, and determine the required size of the reservoir to achieve lifetime specifications. This design tool is available without charge from CCR's web site [9].

CCR performed experiments during the Phase II program to measure barium diffusion rates. Figure 3 shows the test chamber for these measurements. The cathode is mounted in front of a quartz crystal that controls an oscillator. As barium is deposited on the crystal, the amount is determined by the shift in oscillator frequency. Figure 4 shows a plot from one of these measurements.

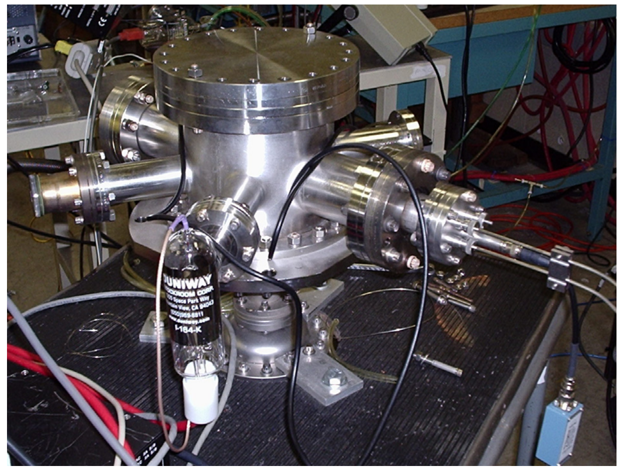

Figure 3. Test chamber for measuring barium diffusion rate and sample measurement

This task included systematic measurements of barium diffusion rates at various temperatures to determine the relationship between barium pressure and emission current density and operating temperature. The experimental measurements confirmed the accuracy of the theoretical predictions used in the GUI-based design tool. The design tool underestimates the diffusion rate by approximately 5%. This provides a margin of error for designers. This insures there will be sufficient barium diffusion to the surface to achieve the design requirements, even in the event that some pores are blocked, as may occur during surface machining.

The diffusion rate is one of two parameters that determines lifetime for a particular reservoir volume. The other important parameter is the barium monolayer evaporation rate from the emission surface. Ideally, the diffusion rate of the emitter cap will precisely match the monolayer evaporation rate from the surface. This will ensure that there is no excess barium deposited on adjacent surfaces, the monolayer is maintained for uniform emission, and the lifetime of the reservoir is maximized. Jensen et al. analyzed the barium evaporation rate for barium tungsten dispenser cathodes [7]. During the Phase II pro-

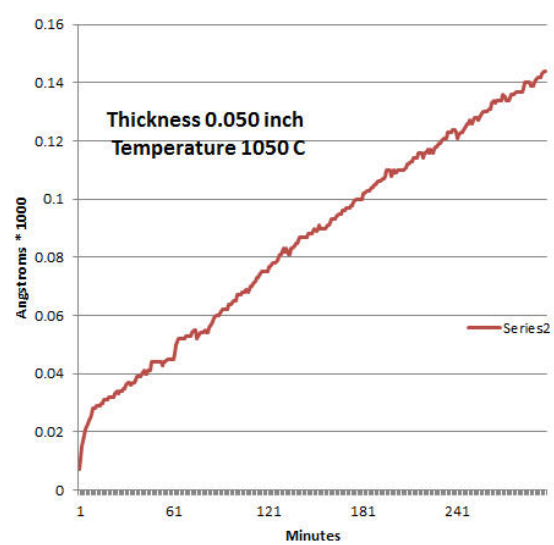

Figure 4. Diffusion measurements for 0.050 inch thick emitter at 1050C

gram this formulation was added to the design program to facilitate matching the diffusion rate with the evaporation rate.

2.2. Investigate alternative materials

The Phase I program investigated alternative reservoir materials to reduce the cathode work function. Cesium appeared to provide a lower work function, but the diffusion rate was not controlled and excessive deposition occurred on adjacent surfaces. Ytterbium did not appear to provide any improvement in performance over barium. While neither material demonstrated the desired performance, they did validate the simplicity involved in testing materials in the reservoir cathodes. It only requires that the material be mixed with appropriate constituent materials and loaded into the reservoir cavity.

During the Phase II program, researchers in China reported on efforts to increase migration of scandate from subsurface regions [10]. They developed a specific compound containing the scandium that appeared to provide the necessary mobility to replenish the surface from a reservoir. CCR proposed to team with this group to develop a CPR cathode configuration containing this compound. Unfortunately, there were insufficient resources in China to pursue this development. If the situation changes, CCR indicated a strong interest in collaborating.

Further research on alternative materials did not indicate potential for improved performance over the standard barium-calcium-aluminate mixture. CCR received two DOE Phase I awards to investigate cesium as a reservoir material for photocathodes, and one of those is in progress [11, 12]. CCR, in collaboration with the University of Maryland, demonstrated an increase in cesitated tungsten photocathode lifetime exceeding two orders of magnitude. The new program is incorporating the reservoir technology for photocathodes operating with higher quantum efficiencies.

2.3. Investigate improved winding and sintering techniques

The Phase II program optimized both the winding and sintering procedures for the tungsten wires constituting the controlled porosity material. Ron Witherspoon, Inc. (RWI) led the effort to improve the winding, and Semicon Associates, Inc. developed the improved sintering process.

2.3.1. Improved winding

Fabrication of the controlled porosity material begins by winding the tungsten wire on a moly spool such that a close packed, hexagonal arrangement of wires is achieved. This is a challenging process, since the diameter of the wire is only 20 microns, and the tension and control of the wire requires a high level of precision. Prior to the Phase II program, RWI used a $500K electro-discharge machine for the winding. While this machine was not designed for this purpose, it provided a high level of precision. Since its prime purpose was machining, it could not be optimized for winding.

RWI contracted with a specialized vendor to reconfigure and deliver equipment specifically designed for precision wire winding. This required special development by both the vendor and RWI, since the equipment was not originally designed to handle 20 micron diameter wire. RWI successfully designed and built specialized fixtures to control the wire tension. This allowed a significant improvement in the uniformity and consistency of the wire during the winding process. A typical winding operation will use approximately 10,000 meters of wire for a single winding. Figure 5 shows a photograph of the winding machine.

Figure 5. Machine for winding 20 micron diameter tungsten wire for controlled porosity material

Acquisition of a dedicated winding machine also allows winding of larger spools with high precision. Cathodes can now be fabricated with four times the surface area than before. This increases opportunities for the cathodes. CCR used this new capability to build a cathode array for a 10 MW, L-Band, Annular Beam Klystron [13].

RWI also developed improved spools for winding. The original spools were made in two sections with one side and the internal structure consisting of one part, and the second side comprising the second part. These were mechanically bonded with moly screws. Figure 6 shows a photograph of this type spool.

Bonding two parts to form the spool proved unsatisfactory. Because of issues with the screws, the spools could only be used 2-3 times.

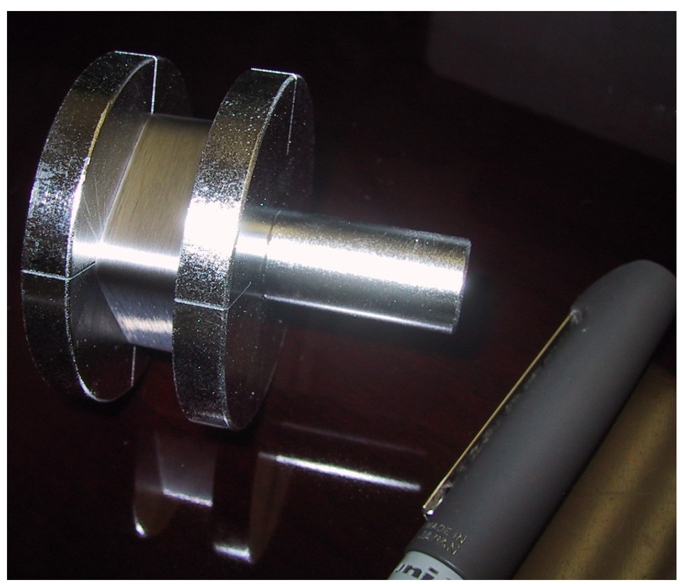

Figure 6. Early version of moly spool used for winding tungsten wire

Either the screws became permanently bonded, requiring destruction of the spool to retrieve the sintered wire, or they failed, resulting in loss of the winding.

The new design uses a spool fabricated as a single part. The sintered wire is removed by making an EDM cut at each corner. The slots for these cuts can be seen in Figure 6. The new design also includes chamfers near the outer edges of the spool. This provided additional compression of underlying wires, which improves sintering. The new spools provide more than five windings before the inner layer of wires begin to bond to the moly. RWI will explore skim cutting the moly to renew the surface. If successful, this will improve the process and reduce the cost of creating the windings.

2.3.2. Sintering

Once the wires are wound on the moly spool, high temperature sintering bonds the individual wires to create a solid structure. The sintered process was described by B.H. Alexander and R.W. Ballufi in 1957 [14]. They investigated the sintering of copper wires wound on a circular spool and fired to various stages of sintering. These stages are illustrated in Figure 7. Alexander and Ballufi demonstrated that the sintered material reaches a stable stage where the pores become circular. Additional sintering has no further impact on the pore shape.

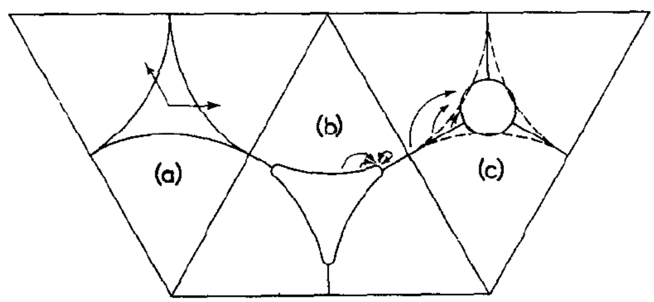

Figure 7. Stages of sintering. Image *(a)* is prior to sintering showing wires forming a pore. Image *(b)* is and intermediate stage and image *(c)* is when the material is fully sintered.

During the program, CCR reviewed literature on sintering [15 - 20]. The information indicates that significantly more time is required to fully sinter tungsten, on the order of 50-70 hours. Prior to the Phase II program, the wire was sintered at 2075^{o} C for 75 minutes. Semicon Associates, Inc., a subcontractor on the program, provided state of the art sintering furnaces and operational personnel. They took the lead in exploring alternative sintering schedules providing more robust structures.

The Phase II program determined the optimum sintering procedure based on performance and cost. Spools are routinely sintered that are extremely robust and immune to splintering and cracking. This has significantly improved machining of the material into structures for reservoir cathodes.

2.4. Develop fabrication techniques for large diameter cathodes

The program investigated issues impacting the size of cathodes. The theoretical development in Task 1 indicated that cathode emitters should be thicker than anticipated to properly match the barium diffusion rate with the evaporation rate from the surface. This significantly impacted cathodes operating at current densities less than 10-15 A/cm^2, since increasing the thickness of the emitter increases the mechanical strength and allows larger diameter emitters.

It was anticipated that the program would investigate the impact of different wire sizes on cathode strength. Investigations during the program indicated, however, that the 20 micron diameter wire was the largest size appropriate for standard thermionic cathodes. Many applications, particularly those focused on higher frequency devices, would obtain better performance with smaller diameter wire. While 10 micron diameter wire is available, the current equipment is not configured to use it. Acquisition of a dedicated winding machine provides the opportunity to explore this opportunity should a commercial demand arise. At this point, however, applications receive acceptable performance from cathodes fabricated with 20 micron diameter wire.

A common technique for achieving larger electron emission surface with smaller cathodes is to use multiple emitters. When the resultant electron beams travel down separate beam tunnels, this has the added advantage of lowering the required beam voltage. Lower voltage increases efficiency and bandwidth in klystrons. CCR applied this technique to an X-Band klystron for a radar application. Fifteen individual cathodes were arranged in two concentric circles. These cathodes operate with an emission current density of 31 A/cm^2. Figure 8 shows the cathode arrangement and a photograph of the completed gun.

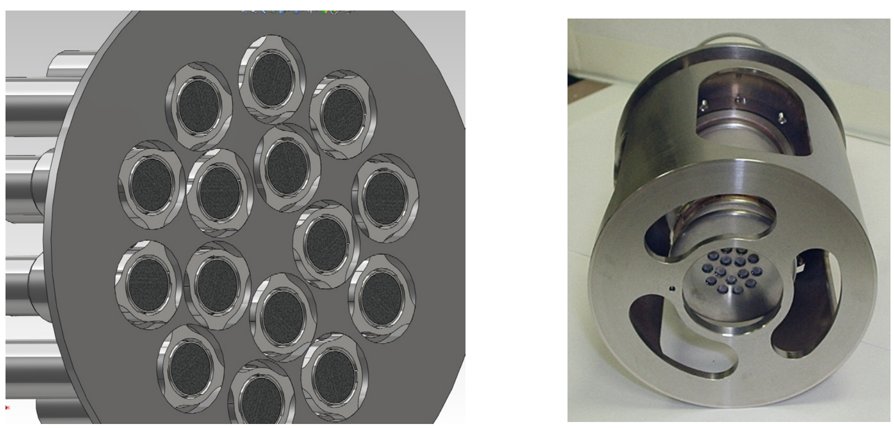

Figure 8. 15-beam gun for a radar application. The left image shows the arrangements of cathodes, and the right photo shows the completed electron gun.

The program developed techniques to fabricated larger cathodes by bonding multiple segments of smaller subassemblies. The initial project involved building twelve arc segments into a magnetron injection gun (MIG) for a 28 GHz gyrotron. This was a collaborative effort with Karlsruhe Institute of Technology (KIT) in Germany. CCR is building the MIG, and KIT will install it into an experimental gyrotron and measure the performance. Ultimately, KIT will use the gyrotron to study the impact of asymmetrical electron beams on gyrotron performance [21, 22].

Figure 9 shows a solid model of the segmented MIG. Note that the individual segments consists of trapezoidal segments angled away from the device axis. This is typical for gyrotron guns, where the emitted electrons must cross magnetic field lines to obtain the transverse velocity required for energy extraction. Figure 10 shows a drawing of one segment with the individual components identified. The KIT application required electrical isolation between each segment, so the heater and cathode leads must be separated from those of other segments. Some thermal isolation is also provided between segments. This will allow researchers to individually control and monitor the current from each segment.

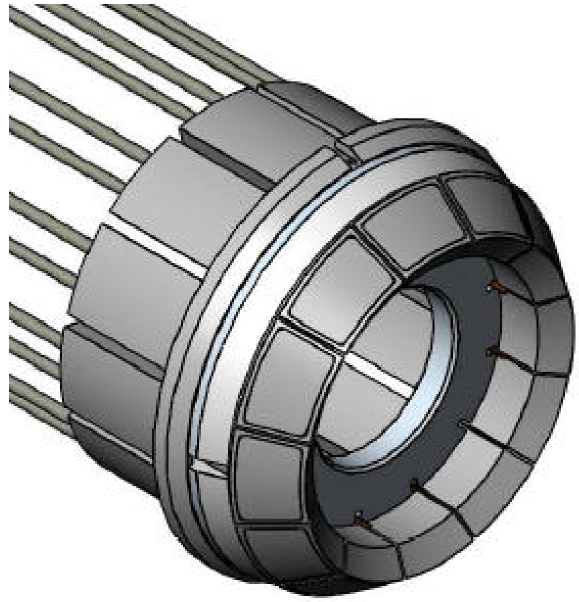

Figure 9. Solid model of segmented MIG

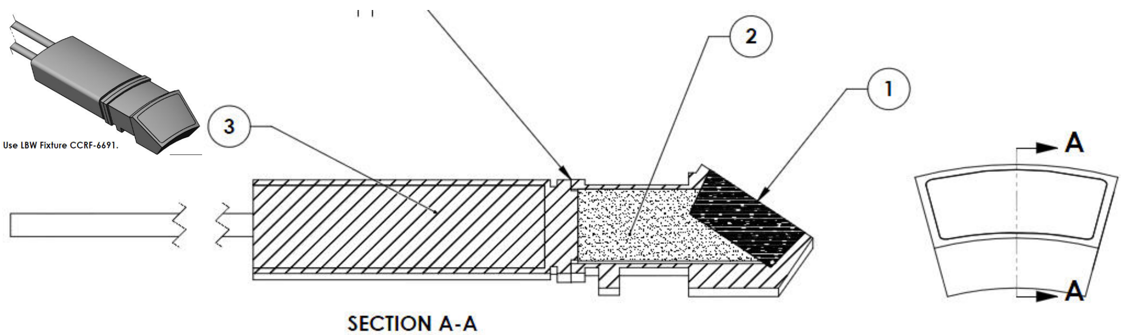

Figure 10. Sliced drawing of MIG segment. Components are (1) emitter, (2) barium-calcium-aluminate reservoir, (3) heater.

The challenge was fabricating and assembling these small components. The emitters are approximately 0.11 inches by 0.55 inches in cross section. Figure 11 shows photographs of the emitter assembly and a complete segment assembly. Eight of the twelve segments required for the MIG are complete and parts are being fabricated for the remaining four. Of the initial order, four segments failed during assembly. The most common failure was cracking of the moly reservoir. One segment was lost when a heater lead failed. Replacement parts are anticipated in the next few weeks, and the gun is schedule for delivery by March 1, 2014.

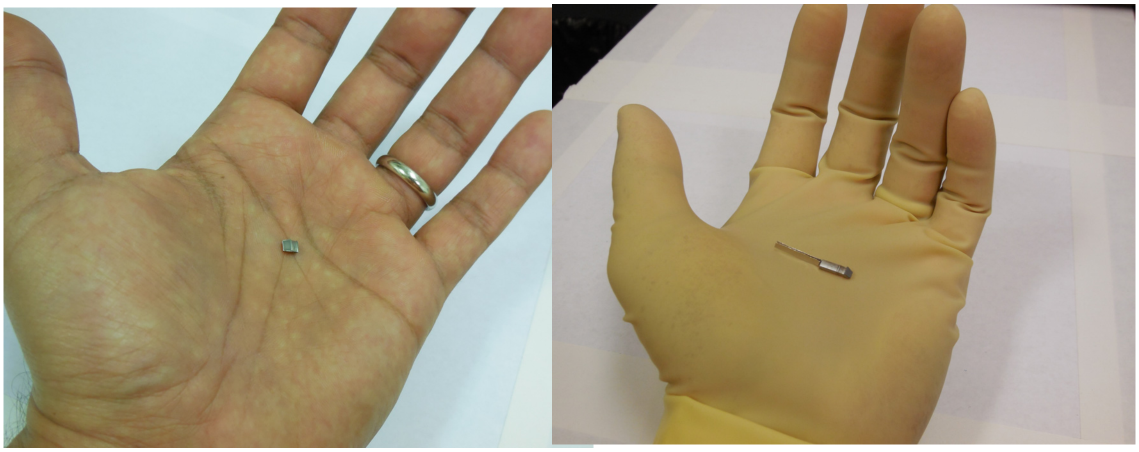

Figure 11. Photographs of MIG emitter (left) and complete segment assembly (right).

A similar techniques was developed for an L-Band, Annular Beam Klystron (ABK) [13, 23]. This cathode uses larger segments fabricated with the new wire winder at RWI. This is currently the largest cathode design using CPR cathodes. The outer

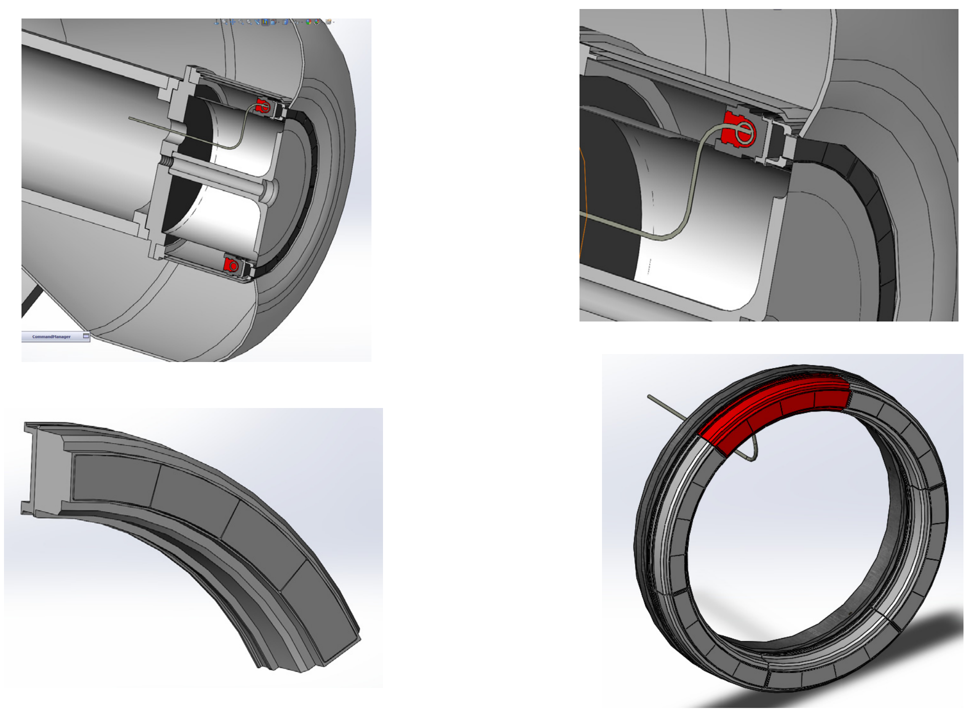

Figure 12. Solid model images of 10 MW annular beam klystron electron gun. From upper left, the images proceeding clockwise show successively zoomed images of the cathode configuration.

diameter of the annular cathode ring is 2.8 inches, and there are twenty four emitter segments in the entire cathode assembly. Four segments are brazed together in each of six subassemblies. This is the first design where sintered wire segments are brazed to each other. All previous assemblies used sintered segments brazed into moly structures.

CCR also developed improved techniques for brazing the emitter segments in the reservoirs. This process involves machining the emitter to the correct diameter and brazing into a counter bore in the reservoir. The depth of the counter bore determines the final thickness of the emitter, which sets the barium diffusion rate. Following the braze, the excess emitter is trimmed to the top of the counter bore and discarded. This process is illustrated in Figure 13. This resulted in significant waste of emitter material. The excess emitter could not be used because braze alloy flowed up the side of the emitter to the exposed surface and closed pores.

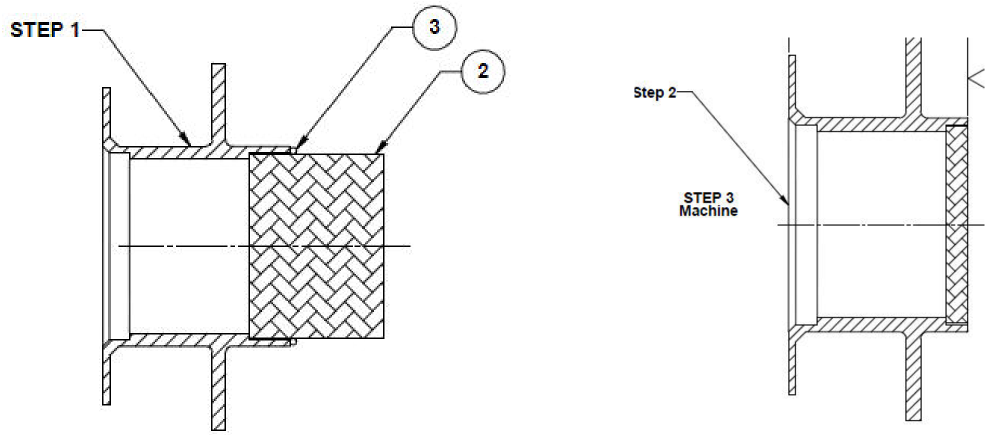

Figure 13. Process for creating reservoir assembly. Item 2 is the emitter, and item 3 is the reservoir cup. The emitter is brazed to the cup in Step 1 and trimmed to the proper thickness in Step 2.

In the new process, reservoir cups are brazed to both ends of the emitter in the same furnace operation. This avoids the issue of braze flow blocking pores and reduced the amount of emitter material required by more than half. The emitter segments can be shorter, since there are no issues with the alloy flow. Once brazed, EDM parts the two assemblies to complete the operation. This process is shown in Figure 14 for the ABK cathode segments, and Figure 15 shows a photograph of two of the six cathode segments for the klystron.

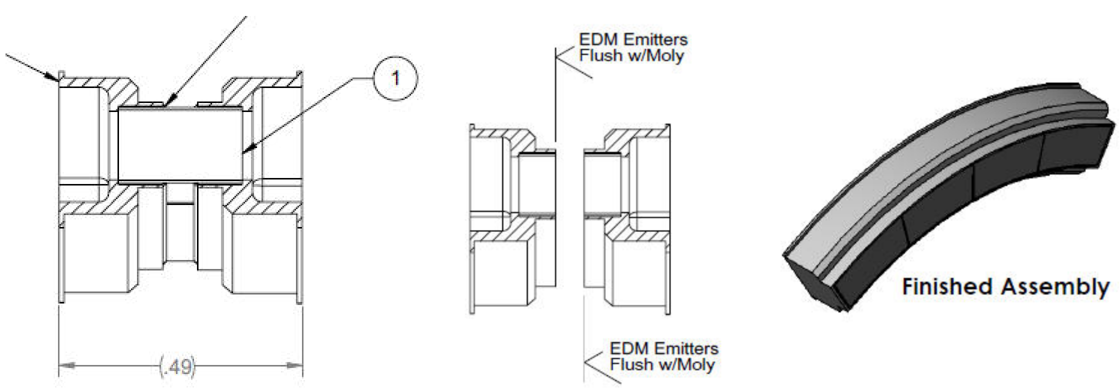

Figure 14. Improved process for brazing reservoir assemblies. The cross hatched part is the reservoir cup. Item 1 is the emitter material. The arrow points to one location for the braze powder.

Figure 15 shows two of the six cathode segments for the klystron. Each segments consists of four individual emitters brazed together. These segments were assembled using a new process where both segments were brazed as a single assembly, then sliced apart using EDM. This significantly reduced the emitter material required as well as insuring that pores would not be blocked by braze alloy flow.

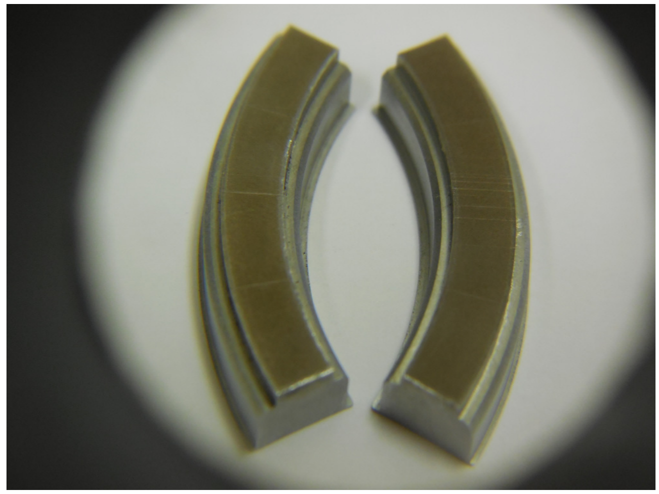

Figure 15. Two of six cathode subassemblies used in an annular beam klystron. Each of these segments consists of four individual emitters.

This klystron is designed to produce 10 MW or RF power at 1.3 GHz. The cathodes will operate at 16 A/cm^2, which eliminates beam compression in the gun. The cathodes provide enabling technology for the development of this klystron. If the klystron is successful, it will cost approximately half that of competing technology.

CCR also improved techniques for developing smaller cathodes. These can be especially problematic, since the reduced number of pores and the close proximity of braze alloy invariably leads to pore obstruction. CCR encountered this problem when cathodes were fabricated for a 100 GHz backward wave oscillator, where the emitter diameter was only 0.024 inches. When the emitter was brazed, approximately 1/2 of the pores became obstructed.

This issue was eliminate by removing brazing as a bonding process. Instead, the emitter was captured with a moly sleeve laser welded to the assembly. This geometry is illustrated in Figure 16. The emitter incorporates a step change from a large diameter that resides within the moly structure to a smaller diameter than extends through a cylindrical section forming the emitter. A moly sleeve clamps the larger diameter section against the interior face of the moly cup. Although there is no bonding of the larger diameter section to the moly, the leak path for barium

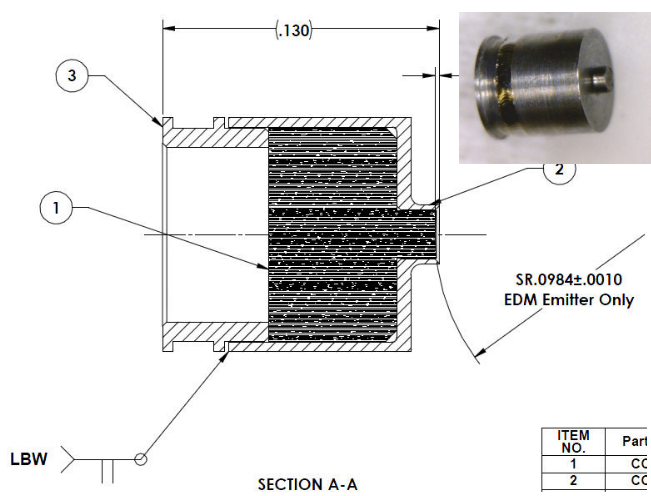

Figure 16. Capture technique for assembling small cathodes

around the periphery is far longer than through the pores of the emitter. Additional compression of the structures is achieved as the assembly cools from the welding process.

CCR is continuing to explore additional opportunities for CPR cathodes. Designs were generated for a 5 MW, grid-pulsed, X-Band klystron for light source applications. The design includes multiple cathode segments with grid structures positioned near the boundaries. This would provide high current density operation without excessive beam interception that would destroy the grid.

CCR will continue to investigate new applications for CPR cathodes.

2.5. Build cathodes and experimentally measure the performance

CCR designed and built an emission microscope to analyze cathode performance and obtain detailed information about the emission surface. The microscope consists of a focusing lens, anode, vertical and horizontal deflection plates, and a current probe. The geometry acts similar to a camera where the emission from the cathode surface is focused to a point and imaged over a larger area downstream. The deflection plates sweep this image past the probe which measures current over a 0.002 inch diameter region. The resultant magnification allows analysis of the emission surface to resolution of several microns. Figure 17 shows the geometry.

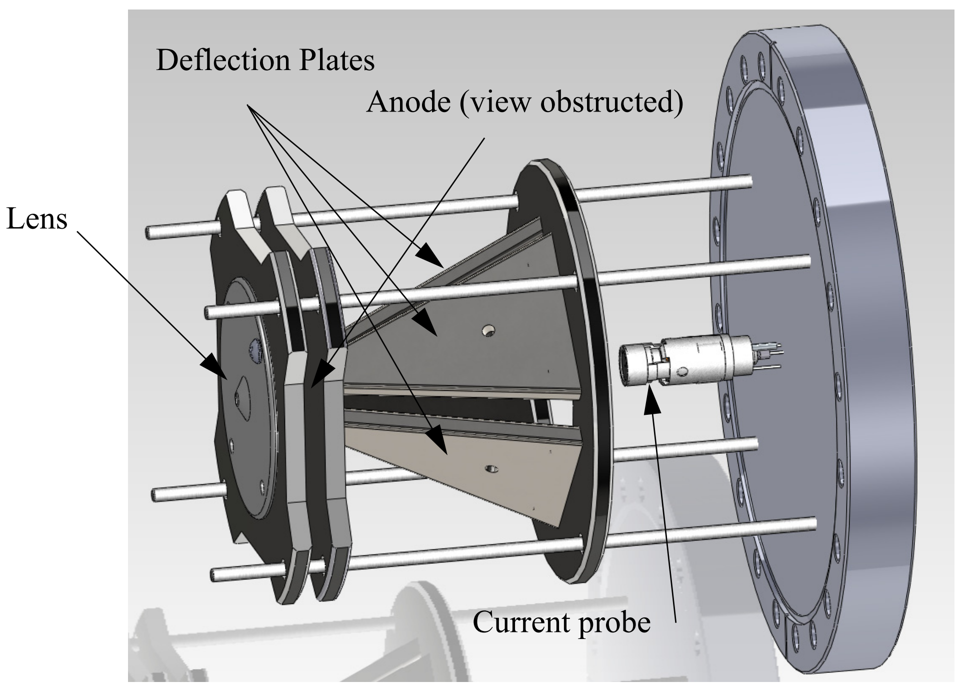

Figure 17. Solid model of the emission microscope

The design was generated using CCR's Beam Optics Analyzer (BOA) code [24 - 27]. The designed determined the position of various electrodes and the voltages required to generate the desired cathode current and sweep he downstream image past the current probe. Figure 18 shows images from the computer simulations.

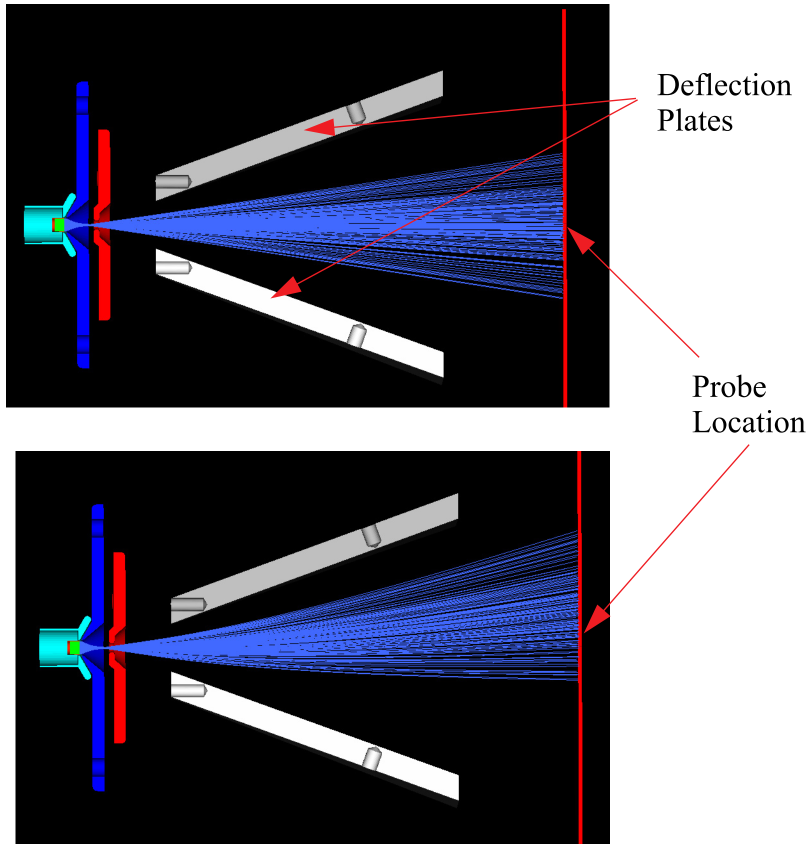

Figure 18. Computer simulations of emission microscope

Figure 19 shows a photograph of the emission microscope components inserted into the vacuum envelope. These are mounted on a conflat flange, so the test cathode can mounted and the lens and anode spacings easily adjusted.

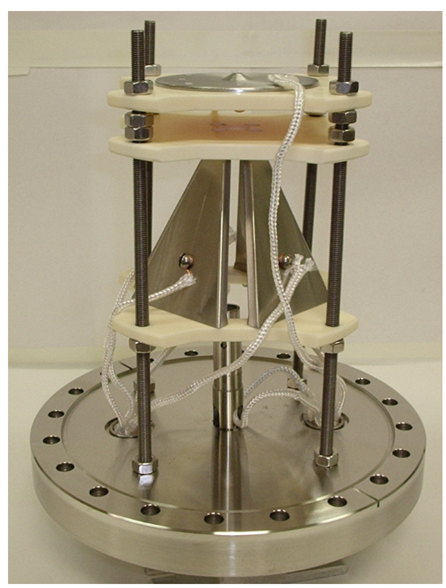

Figure 19. Photograph of emission microscope showing lens, deflection plates, and current probe

Figure 20 shows the complete test system. The high voltage power supply generates pulses between 1 and 10 microseconds at a maximum repetition rate of 10 Hz. The voltage is adjustable from 3 to 20 kV and maximum current is 5 A.

The emission microscope and high voltage power supply are computer controlled, as is data acquisition. A graphical interface allows the user to easily modify the test process. Once operational parameters are set, the computer software automatically performs successive sweeps of the electron beam past the probe until the entire beam is sampled. 3D plots can then be generated of the beam current profile. Figure 21shows several of the GUI screens.

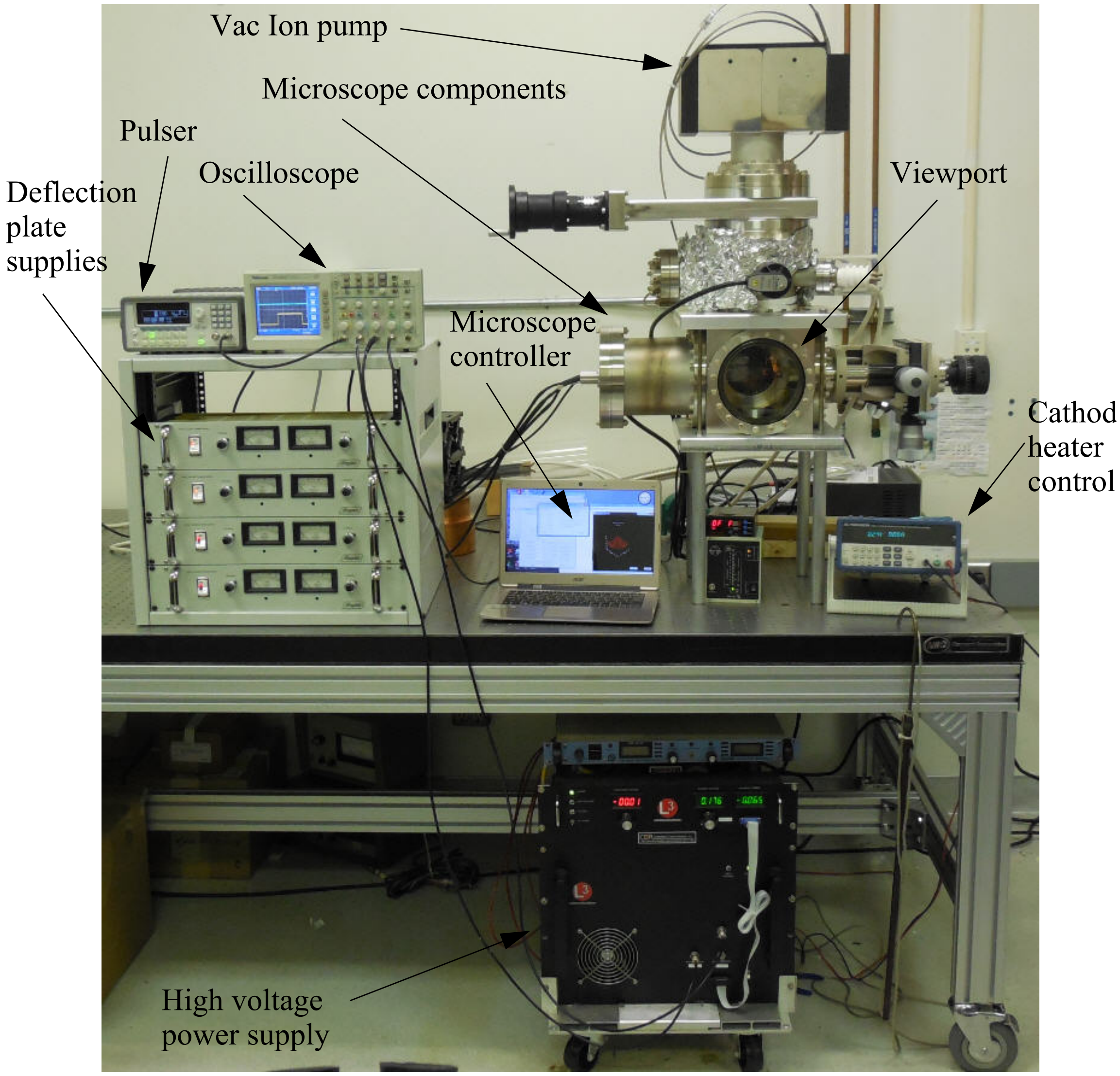

Figure 20. Emission microscope and associated equipment

3. Summary

The program accomplish all the proposed tasks. The design and fabrication process is well established with improved quality and reduced cost. New equipment and processes were implemented that improved both the wire winding and sintering. New assembly techniques extended applications to both smaller and larger cathodes. These applications include small cathodes in a 100 GHz Backward Wave Oscillator; a 15 beam, X-band multiple beam klystron; and a C-Band, 18-beam, multiple beam klystron. Larger cathodes were implemented into a 12-segment, magnetron injection gun for a 28 GHz gyrotron, and a 10 MW, L-Band, Annular Beam Klystron.

The new cathodes are enabling a new generation of RF sources that would not be practical with conventional cathodes, including the applications just mentioned. CCR will continue to seek new opportunities for the cathodes and pursue improvements in design, fabrication, assembly, and operation.

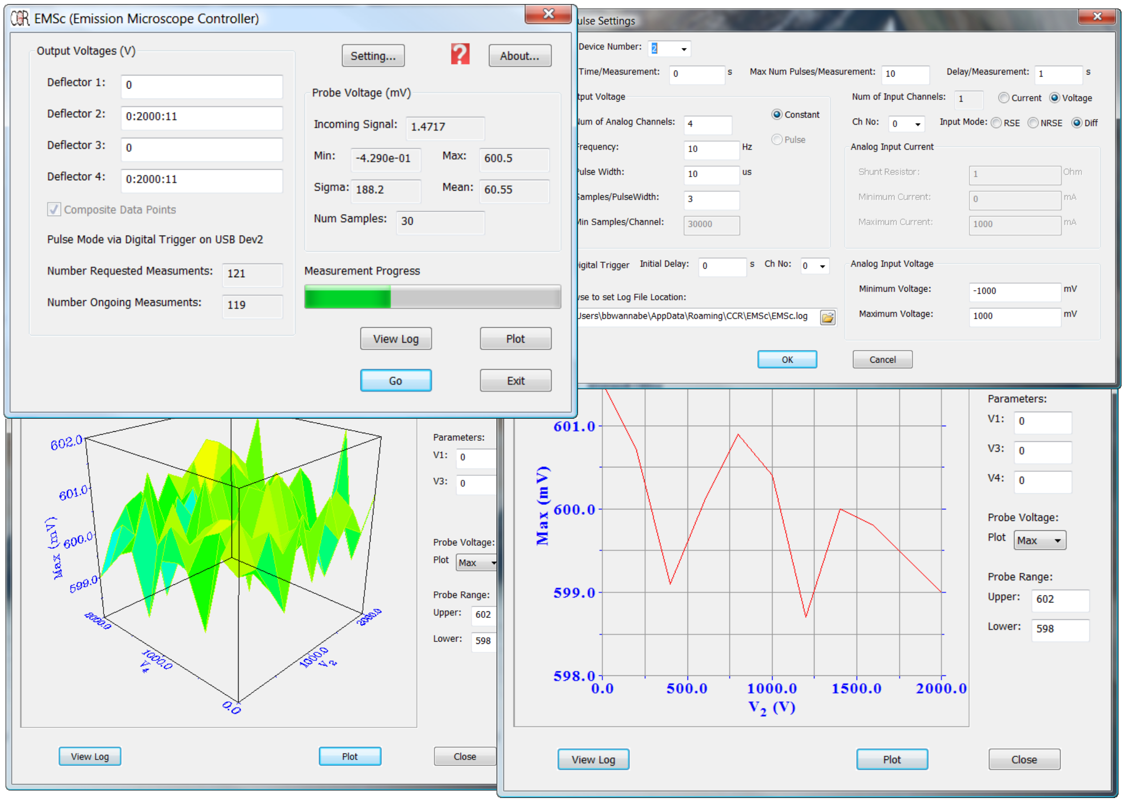

Figure 21. Sample screens from emission microscope graphical user interface

4. References

[1] Improved Magnetron Injection Guns for Gyrotrons, U.S. Dept. of Energy Grant No. DE-FG02-04ER83918, Final Report, October 2007.

[2] 8.R.L. Ives, L.R. Falce, S. Schwartzkopf, and R. Witherspoon, “Controlled Porosity Cathodes from Sintered Tungsten Wires, IEEE Trans. On Electron Devices, Vol. 52, No. 12, pp. 2800-2805, December 2005.

[3] Subcontract from Northup Grumman Corporation under DARPA HiFIVE program contract W911NF-08C-0051, August 2008 through May 2009.

[4] R. Lawrence Ives, Senior Member, IEEE, Louis R. Falce, George Miram, George Collins, “Controlled Porosity Cathodes for High Current Density Applications,” IEEE Trans. Plasma Sci., Special Edition on High Power Microwave Sources, Vol. 38, No. 6, pp. 1345-1353, June 2010.

[5] “Controlled porosity elevates performance, lifetime of cathodes,” R&D Magazine, Vol. 53, No. 5, September 2011.

[6] L. Falce, R.L. Ives, "Sintered Wire Cathode," U.S. Patent No. 7,545,089, June 9, 2009.

[7] K.L. Jensen, Y.Y. Lau, and B. Levush, "Migration and Escape of Barium Atoms in a Thermionic Cathode," IEEE Trans. Plasma Sci., Vol. 28, No. 3, pp. 772-781, June 2004.

[8] Z. Pan, K. Jensen, E. Montgomery, "Modeling the resupply, diffusion, and evaporation of cesium on the surface of controlled porosity dispenser photocathodes," J. of Appl. Physics, Vol. 114, No. 10, pp. 104906 - 1044906-14, 2013.

[9] http://www.calcreek.com/products.html

[10] Yiman Wang et al, "Development of Scandate Cathode and its Prospect_ a review," Intern. Vacuum Electronic Sources Conference, Monterey, CA 2012.

[11] Robust, Long Life Photocathodes, DOE Grant No. DE-SC0006208, June 2011 through March 2012.

[12] Robust RF Photocathodes, DOE Grant No. DE-SC0009583, February 2013 to November 2013.

[13] "10 MW, L-Band Klystron for Accelerators," U.S. Department of Energy SBIR Grant No. DE-SC0006213, June 2011 through April 2014.

[14] B.H. Alexander and R.W. Balluffi, Acta Met., 1957, 5 (11), 666-677.

[15] Sintering of Wire Compacts by A. L. Pranatis and L. Seigle, Above proceedings pp 53-72.

[16] Sintering in the Presence of a Liquid Phase by F. Eisenkolb, Above proceedings pp 75-95.

[17] The Nickel Activated Sintering of Tungsten by J. H. Brophy, L. A. Shepard and J. Wulff, Above Proceedings pp 113-134.

[18] The Fundamental Principles of Powder Metallurgy by W. D. Jones, Edward Arnold Publishers Limited, London.

[19] Powder Metallurgy Principles and Applications by F. V. Lenel, Metal Powders Industry Federation, Princeton, NJ.

[20] Powdered Metals Technology by John McDermott, Noyes Data Corporation, Park Ridge, NJ, London England.

[21] A. Malygin et al, "Analysis of mode competition in 10kW/28GHz gyrotron," Intern. Vacuum Electronics Conf., Paris, France, May 2013

[22] J. Jelonnek et al, "KIT Gyrotron Development for Future Fusion Applications," 38th Intern. Conf. Infrared, Millimeter and THz waves, Mainz, Germany, September 2013.

[23] M. Read et al, “Design and Fabrication of a 10 MW, L-Band, Annular Beam Klystron,” North American Particle Accelerator Conference, Pasadena, CA, September 2013.

[24] CCR Inc., Development of a Finite Element, Adaptive Mesh Charged Particle Code, U.S. Dept. of Energy Grant No. DE-FG-03-00ER82966, Sept. 2000 to June 2003.

[25] T. Bui et. al., Code Development of a 3D Finite Element Particle-In-Cell Code with Adaptive Meshing, IVEC, Noordwijk, The Netherlands, 2005.

[26] T. Bui et. al., An Advanced simulation Code for Modeling Inductive Output Tubes, Phase I Final Report, http://www.osti.gov/scitech/biblio/1039151, 2013.

[27] Beam Optics Analyzer is a commercial code developed and marketed by Calabazas Creek Research, Inc. Additional information is available at www.calcreek.com.